Production of exotic composite quarks at the LHC

O. Panella, R. Leonardi, G. Pancheri, Y. N. Srivastava, M. Narain, and U. Heintz

Production of exotic composite quarks at the LHC

O. Panella,[1] R. Leonardi,[2, 1] G. Pancheri,[3] Y. N. Srivastava,[2] M. Narain,[4] and U. Heintz[4]

[1]*Istituto Nazionale di Fisica Nucleare, Sezione di Perugia, Via A. Pascoli, I-06123 Perugia, Italy**

[2]*Dipartimento di Fisica e Geologia, Università degli Studi di Perugia, Via A. Pascoli, I-06123, Perugia, Italy*

[3]*Laboratori Nazionali di Frascati, INFN, Frascati Italy*

[4]*Physics Department, Brown University, Providence, USA*

We consider the production at the LHC of exotic quarks U^+ of charge $Q = +(5/3)e$ and D^- of charge $Q = -(4/3)e$ of mass m_* arising in a composite fermion scenario characterized by a compositeness scale Λ. Such states are predicted in composite models of higher isospin multiplets ($I_W = 1$ or $I_W = 3/2$). Given their exotic charges (such as 5/3), their decays proceed through the electroweak interactions. We compute decay widths and rates for resonant production of the exotic quarks at the LHC. Partly motivated by the recent observation of an excess by the CMS collaboration in the $e\not{p}_Tjj$ final state signature we focus on $pp \to U^+ j \to W^+ + j\,j \to \ell^+\not{p}_Tjj$ and then perform a fast simulation of the detector reconstruction based on DELPHES. We then scan the parameter space of the model ($m_* = \Lambda$) and study the statistical significance of the signal against the relevant standard model background (Wjj followed by leptonic decay of the W gauge boson) providing the luminosity curves as function of m_* for discovery at 3- and 5-σ level.

I. INTRODUCTION

The idea of a further level of compositeness, i.e. that quarks and leptons might not be truly elementary particles [1] but are instead bound states of some as yet unknown entities has been investigated phenomenologically since quite some time back [2–7]. One immediate consequence of this composite scenario is of course that at some high energy scale, the compositeness scale Λ, excited fermions, quarks and leptons, of mass $m_* \approx \Lambda$ are expected. The interactions of such states with the ordinary quarks and leptons have been modeled on the base of the symmetries of the standard model and are of the magnetic moment type [7].

To the best of our knowledge theoretical and phenomenological studies about the production at colliders of such excited states have concentrated on the multiplets of isospin $I_W = 0, 1/2$ [8, 9]. The LHC experiments have produced new interesting results already starting with the early data of Run I providing the stringent bounds on the mass of excited fermions [10, 11], again restricted to isospin assignments of $I_W = 0, 1/2$ for the excited states.

Two of the present authors studied in ref. [12] the weak isospin spectroscopy of excited quarks and leptons showing that the structure of the standard model symmetries allow to consider higher isospin multiplets up to $I_W = 1, 3/2$. As a consequence one finds for instance that the multiplet with $I_W = 3/2$ (quartet) contains exotic states such as quarks U^+ of charge $+5/3e$ and quarks D^- of charge $-4/3e$.

We remind that alternative scenarios beyond the standard model (BSM) like Little Higgs and Composite

Higgs [13] models predict the existence of vector-like quarks [14–17] which are color-triplet spin 1/2 fermions whose left- and right-handed components have the same transformation properties under the SU(2) gauge group. Such models also predict the existence of vector-like quarks with exotic charges usually denoted as $T_{5/3}$ and $B_{-4/3}$ or X and Y [18–20].

Alternative possibilities of high charge high mass quarks, partners of the top quark have also been proposed [21] to be tested at the LHC and events of the type $t\bar{t}W^+W^-$ have been discussed.

In [22] a detailed study of the production at LHC of vector-like quarks with electric charges $Q = +(5/3)e$, $Q = -(4/3)e$ has been reported showing that at a center of mass energy of $\sqrt{s} = 14$ TeV and with 100 fb^{-1} of integrated luminosity a heavy quark mass of 3.7 TeV could be reached.

We may recall recent experimental searches for pair production of vector-like top quark partners of charge $Q = +(5/3)e$ ($T_{5/3}$) at LHC both at Run I [23], where top-quark partners with masses below 800 GeV are excluded at 95% C.L. assuming that they decay to tW, and at Run II [24, 25] where a data set of 2.2fb^{-1} has been used to obtain exclusion limits, at $\sqrt{13}$ TeV, of 960 (940) GeV respectively on the mass of a right-handed (left-handed) $T_{5/3}$.

Experimental searches of compositeness, already with earlier data of Run I of the LHC ATLAS [10] as well as CMS [26] have put lower limits on the mass of excited quarks, respectively $m_* > 1.2$ TeV and $m_* > 1.58$ TeV, from searches in the 2-jet final state. In [27, 28] an experimental search for narrow resonances decaying to di-jets is presented which uses 12.9 fb^{-1} data from Run II of the LHC and excludes excited quarks (with standard isospin and electric charges) with masses below $m_* \approx 5.4$ TeV extending a previous mass limits of $m_* \approx 5.0$ TeV based on a 2.4 fb^{-1} data samples [29]. Similar searches performed

―――――

* (**Corresponding Author**)
Email: orlando.panella@pg.infn.it

by the ATLAS Collaboration with 3.6 fb^{-1} of proton-proton collisions at $\sqrt{s} = 13$ TeV report a heavy quark mass limit of 5.2 TeV [30]. We also quote phenomenological studies of searches at the LHC in the diphoton [31] and γ-jet [32] final state signatures, showing that in the simplified scenario ($\Lambda = m_*$) with an integrated luminosity of $\mathcal{O}(200)$ fb^{-1} excited quark masses up to ≈ 5 TeV can be probed (i.e. observed or excluded) at 3σ level.

Further details about mass limits and searches through other signatures of the excited quarks (and leptons) can be found in the excellent review [33] about Run I, and earlier Run II, searches at LHC for exotic particles.

It is important to realize however that the above strong limits on the masses of the excited quarks do apply within the hypothesis of standard weak isospin assignments ($I_W = 0, 1/2$). Excited quarks belonging to higher multiplets ($I_W = 1, 3/2$) be their electric charge exotic or not, do not couple to the gluon field (which has $I_W = 0$), and thus it is not possible to produce them resonantly via quark-gluon scattering [12] (see also discussion below).

The possibility of excited quarks was suggested in the context of the SSC [5] but only within the hypothesis of isospin singlets and doublets ($I_W = 0, 1/2$). They were then rediscussed at length in [9]. On the other hand, during the early days of the $S\bar{p}pS$ collider [12] the possibility of possible exotic final states within higher isospin multiplets ($I_W = 1, 3/2$) were explored in $p\bar{p}$ collisions. The phenomenology at high energy colliders of the exotically charged excited fermions from a composite scenario with extended isospin multiplets has however been neglected for a long time after they had been pointed out in [12]. Only recently these exotic fermions have received some attention with respect to the lepton sector. Indeed some of the present authors have studied the production at LHC of the doubly charged leptons of the $I_W = 1, 3/2$ multiplets [34, 35]. We should also mention a recent work where the production of the exotic doubly charged leptons at the linear collider has been considered [36] and another one [37] where the authors explore the possibility that the excited neutrino (ν^*) is of the Majorana type and study the corresponding like sign dilepton signature at the LHC. Incidentally the theoretical possibility discussed in [37] has been experimentally searched for by the CMS Collaboration and through an analysis of the 2015 data [38, 39] of Run II a heavy composite Majorana neutrino is excluded up to $m_* \approx 4.35$ TeV for a value of the compositeness scale fixed at $\Lambda = 5$ TeV. Taking up the model in [12], here we focus on the phenomenology of quarks with higher charges, belonging to weak isospin triplets, $I_W = 1$, and quadruplets, $I_W = 3/2$, which contain quarks U^+ with charges $5/3$ as well as D^- with charges $-4/3$ (apart from states U, D with standard quark charges $+2/3$ and $-1/3$). The interest of these excited quarks lies in the possibility that they belong to a family whose first generation particles would be coupled to the u-quarks of the standard model (SM). A peculiar property of the exotic states U^+ of charge $Q = 5/3e$ is that they couple only to the W gauge boson [12]. This
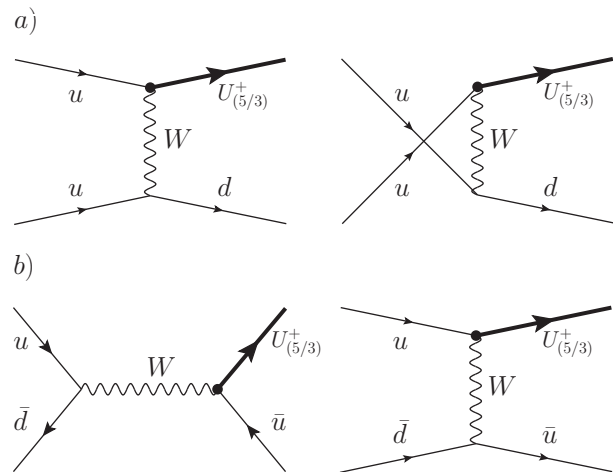

FIG. 1. Example processes of U^+ resonant production in pp collisions: a) the Feynman diagrams for the process $uu \to U^+ d$ showing explicitly W exchange in the t-channel (left) and u-channel (right); b) the Feynman diagrams contributing to the process $u\bar{d} \to U^+ \bar{u}$. On the left the s-channel annihilation. On the right t-channel W exchange. The heavy line is the exotic quark U^+, the heavy dot is the magnetic type coupling characteristic of excited quarks (of electroweak strenght in this case).

can be understood by applying the standard rules of addition of quantum angular momentum and by keeping in mind that that the electroweak gauge bosons ($B_\mu, \boldsymbol{W}$) have respectively $I_W = 0, 1$. Then by recalling that the standard model quarks and leptons appear in isospin singlets ($I_W = 0$) and doublets ($I_W = 1/2$) it is clear that the excited triplet ($I_W = 1$) can only couple to the SM singlet via the gauge field $\vec{W}$. Similarly the ($I_W = 3/2$) multiplet can only couple to the SM doublet again via the $\boldsymbol{W}$ gauge field. By the same token the gluon field which has ($I_W = 0$) cannot couple to a transition current between the higher isospin multiplets ($I_W = 1, 3/2$) and the standard model particles. We conclude these considerations by noting that in our composite scenario the direct coupling of the excited quarks (and leptons) to the SM gauge bosons γ, Z, g, (e.g. $\gamma, Z, g \to q^* \bar{q}^*$) are expected to be highly suppressed by the presence of form factors. This would be very much similar to what happens in nuclear physics with nucleus-antinucleus pair production which is strongly suppressed at $Q^2 \approx m_A^2$ even if the nucleus has a huge electric charge (Ze, with $Z \gg 1$). This implies that the bounds on vector top partners based on pair production of $T5/3$ [23, 24] cannot be applied to the U^+ quark of the present model that are singly produced.

The exotic quarks U^+ have only one decay channel $U^+ \to W^+ u$ with $\mathcal{B}(U^+ \to W^+ u) = 1$. This implies that they could be resonantly produced via the $2 \to 2$ process $uu \to U^+ d$ and hence decay with unit probability to Wu.

We will discuss therefore the production of the *exotic*

excited quarks U^+, D^- at the LHC:

$$pp \to U^+ j \,, \tag{1a}$$
$$pp \to D^- j \,, \tag{1b}$$

and finally assuming the leptonic decay of the W-gauge boson $W \to \ell\nu_\ell$ we concentrate on the $\ell \not{p}_T\, j\, j$ signature(s):

$$pp \to U^+ j \to W^+ j\, j \to \ell^+ \not{p}_T\, j\, j \,, \tag{2a}$$
$$pp \to D^- j \to \ell^- \not{p}_T\, j\, j \,. \tag{2b}$$

The production of the state of charge $Q = 5/3e$ has the largest production cross-section for a pp machine such as the LHC due to the availability of two valence u quarks from the colliding particles. The production of $4/3$ states requires a $\bar{d}$ from the sea and hence its rate is somewhat lower.

We show in Fig. 1 the Feynman diagrams describing some of the parton sub-process contributing Eq. 2a which can produce such exotic final state, $U^+(5/3)$. The processes in Eq. 2b will be given by similar diagrams and will involve at most two valence $d-$quarks in the initial state and thereby the corresponding production cross section are expected to be somewhat smaller than those of the processes in Eq. 2a. Here it will be the dd initiated process that dominates (t and u-channel exchange of a W).

Our phenomenological study of the production of exotic excited quarks in the $\ell \not{p}_T\, j\, j$ channel is particularly interesting in view of the recent claim of the CMS collaboration of having observed excesses, relative to the standard model (SM) background, in the data of the Run I at the LHC at $\sqrt{s} = 8$ TeV in the $eejj$ and $e \not{p}_T\, j\, j$ channels. Indeed the analysis in [40] for a search of right-handed gauge boson, W_R, based on 19.7 fb^{-1} of integrated luminosity collected at a center of mass energy of 8 TeV reports a 2.8σ excess in the $eejj$ invariant mass distribution in the interval $1.8\,\text{TeV} < M_{eejj} < 2.2\,\text{TeV}$. A CMS search [41, 42] for first generation lepto-quarks at a center of mass energy of 8 TeV and 19.6 fb^{-1} of integrated luminosity reported an excess of 2.4σ and 2.6σ in the $eejj$ and $e\not{p}_T jj$ channels respectively.

The absence of a corresponding excess in the $\mu\not{p}_T jj$ channel, as reported in [41, 42], will be difficult to explain solely in terms of heavy exotic quark U^+ or D^- resonant production, via the processes in Eqs (2a,2b) , because the lepton comes from the W gauge boson and thus electrons and muons will have the same yield. However within our composite fermions scenario the signature $\ell\not{p}_T jj$ could get a contribution also from an excited neutrino ν_ℓ^* being produced in association with a lepton $pp \to \ell\nu_\ell^*$ and then decaying as $\nu_\ell^* \to \nu_\ell Z \to \nu_\ell jj$. One could therefore qualitatively explain the fact that the excess is observed only in the $e\not{p}_T jj$ via the combined production and decay of a heavy composite exotic quark U^+ and an excited neutrino by simply assuming that the ν_μ^* has a higher mass than ν_e^*.

We perform a detailed fast simulation of signal and SM background via the DELPHES package [43] and obtain luminosity curves, with the statistical error, as function of the parameter (m_*) at the 3- and 5-σ level. We find that for different values of the integrated luminosity: $(30,300,3000)$ fb^{-1}, commonly used in the study of the LHC Run II ($\sqrt{s} = 13$ TeV) searches, the corresponding mass discovery reach at the 3-σ level is respectively $m_* \approx (3140, 3730, 4260)$ GeV for the more favourable case $I_W = 3/2$.

Our study shows clearly that a full fledged analysis of the upcoming data from the Run II of LHC at $\sqrt{s} = 13$ TeV has the potential of observing the signature or alternatively excluding larger values of the exotic heavy quark masses (m_*) compared to those values already excluded from analyses of Run I [44–46] but applicable only to the standard excited quarks (with non-exotic charges).

The rest of the paper is organized as follows: In Sec. II we review the theoretical composite model; in Sec. III we discuss the heavy exotic quark production cross sections and decay rates; in Sec. IV we discuss the $\ell\not{p}_T jj$ signature and the main associated standard model background and discuss the kinematic cuts needed to optimize the statistical significance; in Sec. V we present the results of the fast simulation obtained through the DELPHES [43] software and present the 3- and 5-sigma luminosity curves in the parameter space; finally Sec. VI gives the conclusions with outlooks.

II. THE EXTENDED WEAK-ISOSPIN MODEL

It is well known that in hadronic physics the strong isospin symmetry allowed to discover baryon and meson resonances well before the observation of quarks and gluons. The properties of the hadronic states could be delineated using the SU(2) and SU(3) symmetries. In analogy with this it may be expected that, for the electroweak sector, the weak isospin spectroscopy could reveal some properties of excited fermions without reference to a particular internal structure.

The standard model fermions have $I_W = 0$ and $I_W = 1/2$ and the electroweak bosons have $I_W = 0$ and $I_W = 1$, so, combining them, we can consider fermionic excited states with $I_W \leq 3/2$. The multiplets with $I_W = 1$ (triplet) and $I_W = 3/2$ (quadruplets) of the hadronic sector include the quarks of exotic charges that are studied in this work:

$$\text{U} = \begin{pmatrix} U^+ \\ U \\ D \end{pmatrix}, \quad \text{D} = \begin{pmatrix} U \\ D \\ D^- \end{pmatrix}, \quad \Psi = \begin{pmatrix} U^+ \\ U \\ D \\ D^- \end{pmatrix},$$

with similar multiplets for the antiparticles. While referring to the original work in [12] for a detailed discussion of all couplings and interactions, we discuss here only the main features of these higher multiplets. We refer to [34] for further details and here we mention only that the
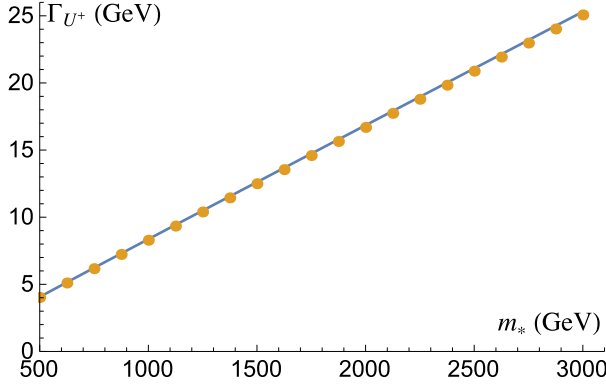
FIG. 2. (Color online) The width of the exotic quark U^+ as a function of its mass. The solid (blue) line is the analytical result in Eq. 8 which is compared with the CalcHEP output, dots (orange) as obtained form the implementation of our model. The agreement is excellent.

higher isospin multiplets ($I_W = 1, 3/2$) contribute solely to the iso-vector current and do not contribute to the hyper-charge current. In order to calculate in detail production and decays of these excited fermions, we need to discuss the nature of their couplings to light fermions and the gauge fields. Because all gauge fields carry no hyper-charge Y, a given excited multiplet couples (through the gauge field) only to a light multiplet with the same Y.

The decay modes and reaction cross sections can be calculated using the following effective lagrangian in terms of the transition currents:

$$\mathcal{L}_{\text{int}}^{(I_W=3/2)} = \frac{g f_{3/2}}{\Lambda} \sum_{M,m,m'} C(\frac{3}{2}, M | 1, m; \frac{1}{2}, m') \times$$
$$\left(\bar{\Psi}_M \sigma_{\mu\nu} q_{Lm'} \right) \partial^\nu (W^m)^\mu + h.c. \qquad (3)$$

$$\mathcal{L}_{\text{int}}^{(I_W=1)} = \frac{g f_1}{\Lambda} \sum_{m=0,\pm 1} \left[\left(\bar{U}_m \sigma_{\mu\nu} u_R \right) + \right.$$
$$\left. \left(\bar{D}_m \sigma_{\mu\nu} d_R \right) \right] \partial^\nu (W^m)^\mu + h.c. \qquad (4)$$

In the above equation g is the SU(2) coupling, f_1 and $f_{3/2}$ are unknown dimensionless couplings expected to be of order one. We will assume them exactly equal to 1 throughout the paper. The mass of the excited fermions m_* will be assumed to coincide with the compositeness scale Λ ($m_* = \Lambda$) and the C'sare Clebsch-Gordon coefficients. We would like to comment here on the need, in our model, of introducing the magnetic moment type transition couplings as in Eqs. (3&4). In our compositeness scenario the interactions of excited leptons and quarks do in general contribute to the e.m. current. This always happens for the excited states of ordinary charges. According to Eqs. (3&4), as detailed in [12], the U (D) quarks of charge 2/3 (-1/3) will contribute with the following interactions:

$$\mathcal{L}_{\text{int. }(U, D)}^{(I_W=3/2)} = \frac{g f_{3/2}}{\Lambda} \left\{ \frac{1}{\sqrt{3}} \bar{U} \sigma^{\mu\nu} d_L \, \partial_\nu W^+_\mu + \sqrt{\frac{2}{3}} \sin\theta_W \bar{U} \sigma^{\mu\nu} u_L \, \partial_\nu A_\mu + \sqrt{\frac{2}{3}} \cos\theta_W \bar{U} \sigma^{\mu\nu} u_L \, \partial_\nu Z_\mu \right.$$
$$\left. + \frac{1}{\sqrt{3}} \bar{D} \sigma^{\mu\nu} u_L \, \partial_\nu W^-_\mu + \sqrt{\frac{2}{3}} \sin\theta_W \bar{D} \sigma^{\mu\nu} d_L \, \partial_\nu A_\mu + \sqrt{\frac{2}{3}} \cos\theta_W \bar{D} \sigma^{\mu\nu} d_L \, \partial_\nu Z_\mu + h.c. \right\} \qquad (5)$$

$$\mathcal{L}_{\text{int. }(U, D)}^{(I_W=1)} = \frac{g f_1}{\Lambda} \left\{ \bar{U} \sigma^{\mu\nu} d_R \, \partial_\nu W^+_\mu + \sin\theta_W \bar{U} \sigma^{\mu\nu} u_R \, \partial_\nu A_\mu + \cos\theta_W \bar{U} \sigma^{\mu\nu} u_R \, \partial_\nu Z_\mu \right.$$
$$\left. + \bar{D} \sigma^{\mu\nu} u_R \, \partial_\nu W^-_\mu + \sin\theta_W \bar{D} \sigma^{\mu\nu} d_R \, \partial_\nu A_\mu + \cos\theta_W \bar{D} \sigma^{\mu\nu} d_R \, \partial_\nu Z_\mu + h.c. \right\} \qquad (6)$$

We note that both the e.m. and the SU(2) currents are evidently conserved due to the anti-simmetry of the tensor $\sigma_{\mu\nu}$. Clearly a current of the type $J_\mu \sim \bar{U} \gamma_\mu P_L u$ would not be conserved as can be easily seen by using the Dirac equation for the two spinors and keeping in mind the mass difference between the excited and ordinary quark.

It is crucial here to recall that an essential point of our model is that the heavy excited quarks are assumed to get their mass not by the Higgs mechanism but through the unknown *preon* dynamics. This means that even prior to SU(2) symmetry breaking by the Higgs field our excited fermions are massive, while all other SM particle will be massless. In this case we should expect also the neutral and charged currents to the W and Z gauge bosons to be exactly conserved as the W and Z are also massless and thus satisfy gauge invariance. This fixes all our transition coupling(s), between the heavy excited states and the light SM particles, to be of the magnetic $\sigma_{\mu\nu}$-type, both for the e.m. current as well as for the SU(2) currents.

At variance with our composite scenario in VLQ models the vector interactions of top partners $T_{5/3}$ and partners with light generation quarks, as described for instance in [47, 48], do not involve the electro-magnetic field (or the gluon) but are restricted to only the W, Z and the Higgs bosons. Here the heavy partners are as-

sumed to get their masses from the Higgs mechanism as usual. Clearly vector-like interactions between a SM fermion and a heavy partner with the photon (gluon) field would violate gauge invariance (see for instance Eq. 2.1 in reference [47]). We also note that in VLQ models the transition magnetic-type interactions with the photon and gluon fields appear as effective couplings at one loop order [47].

There is another fundamental difference between the magnetic moment vs vector couplings to the fermions. For a vector coupling, a left (right) fermion couples to a left (right) fermion; for magnetic moment coupling it is the opposite.

In particular we see that the particles of these higher multiplets with exotic charges interact with the standard model fermions only via the physical W gauge field. For the exotic quark U^+ of charge $Q = +(5/3)e$ belonging to the $I_W = 1$ triplet and the one of the $I_W = 3/2$ quadruplet the relevant interaction lagrangians are respectively:

$$
\mathcal{L}^{(I_W=3/2)}_{\text{int}\,(U^+,D^-)} = \frac{g\,f_{3/2}}{\Lambda} \left[\bar{U}^+ \sigma^{\mu\nu} u_L\, \partial_\nu W^+_\mu \right.
$$
$$
\left. + \bar{D}^- \sigma^{\mu\nu} d_L\, \partial_\nu W^-_\mu + h.c. \right] \quad (7a)
$$

$$
\mathcal{L}^{(I_W=1)}_{\text{int}\,U^+} = \frac{g\,f_1}{\Lambda} \left[\bar{U}^+ \sigma_{\mu\nu} u_R \partial_\nu W^+_\mu \right.
$$
$$
\left. + \bar{D}^- \sigma^{\mu\nu} d_R\, \partial_\nu W^-_\mu + h.c. \right] \quad (7b)
$$

where: $P_L = (1 - \gamma^5)/2$ and $P_R = (1 + \gamma^5)/2$ are the chiral projectors and $\sigma^{\mu\nu} = i\left[\gamma^\mu, \gamma^\nu\right]/2$; as usual g is the SU(2) coupling constant $g = e/\sin\theta_W$; the field U^+ stands for the exotic quark field both for the case $I_W = 1$ and $I_W = 3/2$; u is the u-quark field. The effective Lagrangian in (7) is a dimension five operator and hence one inverse power of the new physics scale (the compositeness scale) Λ appears. In the following phenomenology we will consider the simplified model $\Lambda = m_*$.

With the above interaction Lagrangian we can easily compute the total decay width of the exotic state U^+ of charge $q = (5/3)e$. Indeed as it only interacts via the W gauge boson its only decay channel is $U^+ \to W^+ u$, and:

$$
\Gamma_{U^+} = \Gamma(U^+ \to W^+ u)
$$
$$
= \alpha_{QED}\, \frac{f_{3/2}^2}{\sin^2\theta_W}\, \frac{m_*}{8} \left(2 + \frac{M_W^2}{m_*^2} \right) \left(1 - \frac{M_W^2}{m_*^2} \right)^2 (8)
$$

hence we see that for $m_* \gg M_W$, and assuming $f_{3/2} \sim 1$: $\Gamma_{U^+}/m_* \approx \mathcal{O}(\alpha_{QED})$. This behavior is shown explicitly in Fig. 2 where the width Γ_{U^+} is plotted versus the mass m_*.

We have implemented the interactions of the exotic quarks discussed in section II within the CalcHEP software [49]. This has been done with the help of FeynRules [50], a Mathematica package that from a given model lagrangian produces as output the Feynman rules in a format that can be read by various software tools

such as CalcHEP and Madgraph. we note that the standard model background to the process described in Eq. 1 has been discussed in [51–54].

In Fig. 2 we give a first comparison of the CalcHEP output within our newly implemented model versus an analytical computation of the width of the exotic massive quark U^+. The agreement is excellent.

We conclude this section by commenting briefly on indirect bounds on compositeness available from the literature. The effects of excited leptons on the electron and muon anomalous magnetic moment were studied in [55, 56]. It was found that without chiral symmetry the bounds on the compositeness scale and/or mass ($\Lambda = m_*$) form (g-2) are very tight. However assuming chiral symmetry, which is the case of our model, the bounds become comparable to those from direct searches (at least those available at the time ref. [55, 56]). Current bounds from direct searches at the LHC of the order of the TeV are stronger than those obtainable from g-2. In [57] the authors investigated the one-loop effects of excited leptons (grouped in SU(2) doublets, i.e. $I_W = 1/2$) in the electroweak observables measured on the Z-peak at LEP; the results showed that these effects could not constrain the parameters Λ and m_* beyond the limits from direct searches available at the time. While it would be certainly very interesting to extend the study presented in [55–57] to higher iso-spin multiplets we expect that such indirect bounds would not be much competitive with those from current direct searches at the LHC. Finally we would like to remark that with respect to the flavor structure of our model we assume that the excited quarks are organized in three families like the ordinary quarks. The couplings between excited and ordinary quarks are assumed to be restricted to the same family.

III. PRODUCTION CROSS SECTIONS

The exotic quark U^+ interacts with the ordinary quarks through a typical magnetic type interaction *only via the W gauge boson* and in pp collisions it can be be produced via the first generation sub-processes: (a) $uu \to U^+ d$ (t and u-channel W exchange); (b) $u\bar{d} \to U^+ \bar{u}$ (s and t-channel W exchange) as depicted in Fig. 1. Within the first generation we have the parton sub-processes:

$$
u\,u \to\, U^+ d \to\, W^+ u\,d \quad (9a)
$$
$$
u\,\bar{d} \to\, U^+ \bar{u} \to\, W^+ u\,\bar{u} \quad (9b)
$$

which may be observed in either a final state with 4 jets or 2 jets and W^+ decaying electroweakly. Together with such a high charge member of the mutiplet, the lower charge exotic quark member of the multiplet would also be produced. An exotic excited fermion of charge $Q = -(4/3)e$ may be produced through

$$
d\,d \to\, D^- u \to\, W^- d\,u \quad (10a)
$$
$$
d\,\bar{u} \to\, D^- \bar{d} \to\, W^- d\,\bar{d} \quad (10b)
$$

Similar diagrams to those depicted in Fig. 1 will describe the production of the exotic state D^-. We now discuss the production cross sections of the $2 \to 2$ processes discussed above.

A. Partonic cross section

Following notation and conventions of ref. [12, 36] we give here the basic cross-sections of the partonic sub-processes. The case of the weak isospin $I_W = 1$ is characterized by the absence of interference between $\hat{t}-$ and $\hat{u}-$channel (or $\hat{s}-$ and $\hat{t}-$channel). The partonic cross-section for the processes $uu \to U^+ d$ and $u\bar{d} \to U^+ \bar{u}$ are given by:

$$\left(\frac{d\hat{\sigma}}{d\hat{t}}\right)_{uu \to U^+ d} = \frac{1}{4\hat{s}^2 m_*^2} \frac{g^4 f_1^2}{16\pi} \left\{ \frac{\hat{t}\left[m_*^2(\hat{t} - m_*^2) + 2\hat{s}\hat{u} + m_*^2(\hat{s} - \hat{u})\right]}{(\hat{t} - M_W^2)^2} + \frac{\hat{u}\left[m_*^2(\hat{u} - m_*^2) + 2\hat{s}\hat{t} + m_*^2(\hat{s} - \hat{t})\right]}{(\hat{u} - M_W^2)^2} \right\} \quad (11)$$

$$\left(\frac{d\hat{\sigma}}{d\hat{t}}\right)_{u\bar{d} \to U^+ \bar{u}} = \frac{1}{4\hat{s}^2 m_*^2} \frac{g^4 f_1^2}{16\pi} \left\{ \frac{\hat{s}\left[m_*^2(\hat{s} - m_*^2) + 2\hat{t}\hat{u} + m_*^2(\hat{t} - \hat{u})\right]}{(\hat{s} - M_W^2)^2} + \frac{\hat{t}\left[m_*^2(\hat{t} - m_*^2) + 2\hat{s}\hat{u} + m_*^2(\hat{s} - \hat{u})\right]}{(\hat{t} - M_W^2)^2} \right\} \quad (12)$$

The case of the weak isospin $I_W = 3/2$ is characterized instead by nonzero interferences between $\hat{t}-$ and $\hat{u}-$channel (or $\hat{s}-$ and $\hat{t}-$channel) which had been neglected in ref. [12]. The partonic cross-sections for the processes $uu \to U^+ d$ and $u\bar{d} \to U^+ \bar{u}$ are given by:

$$\left(\frac{d\hat{\sigma}}{d\hat{t}}\right)_{uu \to U^+ d} = \frac{1}{4\hat{s}^2 m_*^2} \frac{g^4 f_{3/2}^2}{16\pi} \left\{ \frac{\hat{t}\left[m_*^2(\hat{t} - m_*^2) + 2\hat{s}\hat{u} - m_*^2(\hat{s} - \hat{u})\right]}{(\hat{t} - M_W^2)^2} + \frac{\hat{u}\left[m_*^2(\hat{u} - m_*^2) + 2\hat{s}\hat{t} - m_*^2(\hat{s} - \hat{t})\right]}{(\hat{u} - M_W^2)^2} \right.$$
$$\left. + \frac{1}{(\hat{u} - M_W^2)} \frac{1}{(\hat{t} - M_W^2)} \left(\hat{s}\hat{t}\hat{u} + \frac{3}{8}\hat{u}\hat{t}m_*^2\right) \right\} \quad (13)$$

$$\left(\frac{d\hat{\sigma}}{d\hat{t}}\right)_{u\bar{d} \to U^+ \bar{u}} = \frac{1}{4\hat{s}^2 m_*^2} \frac{g^4 f_{3/2}^2}{16\pi} \left\{ \frac{\hat{s}\left[m_*^2(\hat{s} - m_*^2) + 2\hat{t}\hat{u} - m_*^2(\hat{t} - \hat{u})\right]}{(\hat{s} - M_W^2)^2} + \frac{\hat{t}\left[m_*^2(\hat{t} - m_*^2) + 2\hat{s}\hat{u} - m_*^2(\hat{s} - \hat{u})\right]}{(\hat{t} - M_W^2)^2} \right.$$
$$\left. + \frac{1}{(\hat{s} - M_W^2)} \frac{1}{(\hat{t} - M_W^2)} \left(\hat{s}\hat{t}\hat{u} + \frac{3}{8}\hat{s}\hat{t}m_*^2\right) \right\} \quad (14)$$

The above formulas have also been checked against the results reported in [36] by means of using the crossing symmetry. The total integrated cross-section corresponding to the above differential cross section is given for the process $u\bar{d} \to U^+ \bar{u}$ (which receives contributions both from the s and t-channels in FIG. 3. One can see that at high energies the integrated cross section rises logarithmically due to the effect of the t-channel W propagator. Also the standard $(1/\hat{s})$ behavior of the cross section is not found because of the magnetic type coupling. The asymptotic form of the integrated partonic cross sections (t-channel) is :

$$\hat{\sigma} = \int_{-\hat{s}+m_*^2}^{0} d\hat{t} \frac{d\hat{\sigma}}{d\hat{t}} \quad (15)$$

$$\underset{\hat{s} \gg M_W^2, m_*^2}{\Longrightarrow} \sim \frac{\pi \alpha_{QED}^2 f_1^2}{\sin^2 \theta_W} \frac{1}{m_*^2} \log\left(\frac{s}{M_W^2}\right)$$

as can also be seen from FIG. 3.

B. Production rates at the LHC

We now present here the production cross sections for the exotic quark U^+ in pp collisions expected at the CERN LHC collider according to Feynman's parton model. The QCD factorization theorem, allows to obtain the hadronic cross section in terms of convolution of the partonic cross sections $\hat{\sigma}(\tau s, m_*)$, evaluated at the partons center of mass energy $\sqrt{\hat{s}} = \sqrt{\tau s}$, and the universal parton distribution functions f_a which depend on the parton longitudinal momentum fractions, x, and on the factorization scale $\hat{\mathcal{Q}}$:

$$\sigma = \sum_{a,b} \int_{\frac{m_*^2}{s}}^{1} \int_{\tau}^{1} d\tau \frac{dx}{x} f_a(x, \hat{\mathcal{Q}}) f_b\left(\frac{\tau}{x}, \hat{\mathcal{Q}}\right) \hat{\sigma}(\tau s, m_*) . \quad (16)$$

In Fig. 4 we show a comparison of the production cross sections of $pp \to U^+ j$ at $\sqrt{s} = 8, 13$ TeV between those obtained with an analytical/numerical computation based on Eq. 16 (solid line) and those obtained from a CalcHEP numerical simulation based on the implemented model (full dots). The left panel of Fig. 4 is for the $I_W = 1$ case while the right panel is for $I_W = 1$.
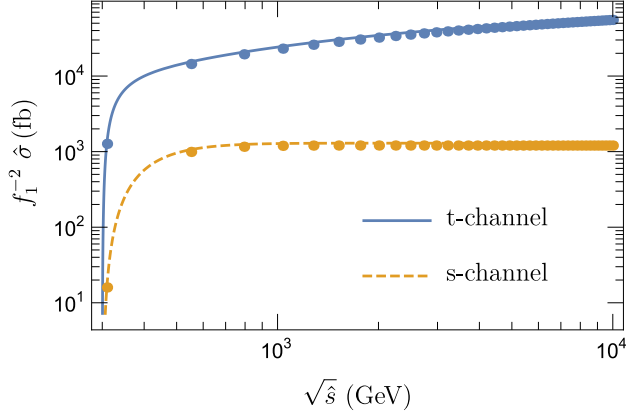
FIG. 3. (Color online) For illustrative purposes we give an example of the parton-parton cross-section as indicated in Eq. 15 (no parton ditribution functions). We show $\hat{\sigma}(u\bar{d} \to U^+\bar{u})$ for $m_* = 300$ GeV for the case of the weak isospin $I_W = 1$ (in this case there is no interference between the $t-$ and $s-$channel) and with a choice of the coupling $f_{1q} = 1$. The solid line (blue) is the dominant t-channel and the dashed line (orange) is the s-channel. The dots are the corresponding values obtained by running the same process in CalcHEP within the model implemented with the help of the FeynRules package. The agreement is excellent, within a few percent.

The integrated hadronic cross sections are further shown in Fig. 5 where we present the results for two different values of the LHC energy, namely $\sqrt{s} = 8, 13$ TeV. In the top panel we show for $\sqrt{s} = 8$ TeV the total integrated cross section for the production of $U^+(5/3)$ and $D^-(4/3)$ for $I_W = 1$ (left) and $I_W = 3/2$ (right). As expected one finds that the production of $U^+(5/3)$ is larger. This is almost entirely due to the fact that producing U^+ involves the subprocess $uu \to U^+d$ i.e. with two valence u-quarks in the initial state. Similar considerations apply to the results at higher energies (bottom panels). For the production of U^+ we have, within the first two generations, the following contributing subprocesses: (a) $uu \to U^+d$; (b) $u\bar{d} \to U^+\bar{u}$; (c) $uc \to U^+s$; (d) $u\bar{s} \to U^+\bar{c}$;

The large mass of the excited leptons/quarks is due to some internal dynamics and not from the Higgs mechanism. Hence, modulo Higgs breaking, the excited fermion mass matrix is SU(2)×U(1) diagonal and flavour diagonal. The flavour changing neutral currents by mixing with light fermions when Higgs breaking occurs are expected to be quite small specially when the mass is very large.

The ordinary charge excited quarks U, D present both in the triplet and quadruplet are therefore mass degenerate with the corresponding U^+, D^- states of exotic charge. As shown explicitly in Eq. (5,6) the U, D states do interact with the SM gauge bosons (W, Z, γ). In particular as detailed in [12] both for the triplet $(I_W = 1)$ and the quadruplet $(I_W = 3/2)$ they interact with the W, Z and γ (for instance they can de-

m_*	U^+	U	$\bar{D}$	$\bar{D}^-$	$\sigma_{\rm tot}(e^+\not{p}_Tjj)$
(GeV)	(fb)	(fb)	(fb)	(fb)	(fb)
500	7782.0	6303.0	2594.0	2679.0	19358.0
1000	1277	978	329.4	357.3	2941.7
1500	344.6	250.30	73.390	90.400	758.69
2000	107.7	74.580	23.370	28.330	233.98
2500	39.05	24.740	8.689	9.1740	81.653
3000	13.5	9.5770	4.043	2.459	29.579
3500	4.281	3.612	1.119	0.7004	9.7124
4000	1.424	1.3470	0.2401	0.2161	3.2272
4500	0.4957	0.4958	0.06098	0.06365	1.11613
5000	0.1799	0.18530	0.01819	0.0211	0.4045

TABLE I. Various contribution to the final state signature $(e^+\not{p}_Tjj)$ from the excited quarks (U^+, U, D, D^-) of the triplets of $I_W = 1$.

cay $U \to dW$, $U \to uZ$, and $U \to u\gamma$) with definite branching ratios [12]. This means that the the states U, D contribute to the Wqq channel, although with a branching ratio $\mathcal{B}(U \to W^+d) \approx 0.22$ as compared to $\mathcal{B}(U^+ \to W^+u) = 1$.

Therefore both for the $I_W = 3/2$ (quadruplet) and the $I_W = 1$ (triplet) we have included the contribution of the states U, D to the W^+qq yield in addition to the one from the the exotic states U^+, D^-. Such contributions are expected to be sizable because the U, D are produced with diagrams similar to those of Fig. 1 but involving all SM gauge bosons (W, Z, γ). In particular diagrams with a t-channel photon exchange strongly enhance the contributions of the (U, D) states. On the contrary other final state signatures of the type Zjj (or γjj) would receive contributions from the ordinary carged states (U, D) but not from the states of exotic charge U^+, D^- since these do not couple to the Z and γ gauge bosons, as shown explicitly in Eq. (7). It turns out that the contributions to the W^+qq yield from U, D, D^- are typically a sizable fraction of the yield from the U^+ of charge 5/3. For instance the (largest) U contribution varies from 80% (30%) at $m_* = 500$ GeV up to $\approx 100\%$ (down to 20%) at $m_* = 5000$ GeV of that from U^+ for $I_W = 1$ $(I_W = 3/2)$. See new Table I (page 7) and Table II (page 8).

IV. SIGNAL AND SM BACKGROUND

The relevant standard model background to our signature is given by electroweak Wjj production followed by the leptonic decay of the W gauge boson, $W \to \ell\nu_\ell$:

$$pp \to Wjj \to \ell\not{p}_Tjj \qquad (17)$$

This SM background is known to be important and has been discussed throughly in the literature. We have simulated it by using the CalcHEP generator.

We would like to address here the main kinematic differences between the signal and the relevant SM background in order to choose suitable cuts for optimizing the statistical significance.
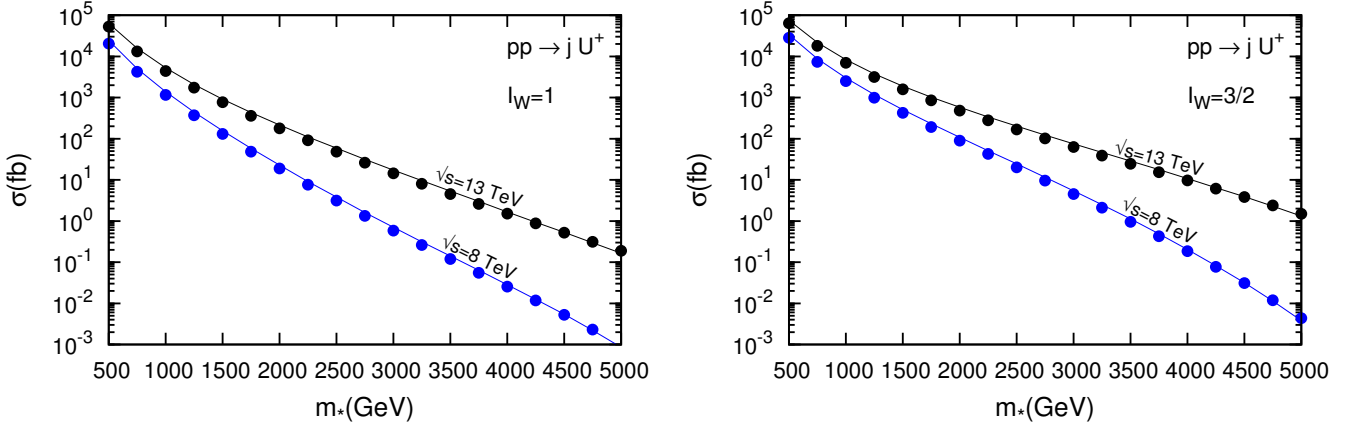
FIG. 4. (Color online) The total production rates of $pp \to jU^+$ at the LHC for two different values of the energy of the center of mass $\sqrt{s} = 8, 13$ TeV and for the two choices of the weak isospin of the exotic states, $I_W = 1$ on the left panel and $I_W = 3/2$ on the right panel. The solid lines refer to the output of our code based on Eq. (16). The agreement with of the output obtained with the model implemented in CalcHEP is within a few percent. Here the factorization and renormalization scale is fixed at $\hat{\mathcal{Q}} = m_*$. The parametrization of the parton distribution function is NNPDF3.0 [58].

m_* (GeV)	U^+ (fb)	U (fb)	$\bar{D}$ (fb)	$\bar{D}^-$ (fb)	$\sigma_{\rm tot}(e^+ \not{p}_T jj)$ (fb)
500	11080	3446.0	1506.0	477.60	16509.6
1000	2240	623.70	151.30	47.46	3062.46
1500	806.3	203.20	28.750	8.8000	1047.05
2000	343.2	82.890	6.3130	1.954	434.357
2500	159.9	40.760	1.7260	0.5253	202.911
3000	60.25	24.130	0.44890	0.15880	84.9877
3500	23.55	8.5430	0.12390	0.053250	32.2702
4000	9.347	2.0480	0.03894	0.018810	11.4527
4500	3.191	0.6354	0.01335	0.006457	3.84621
5000	1.043	0.2034	0.004864	0.002433	1.2537

TABLE II. Various contribution to the final state signature $(e^+ \not{p}_T jj)$ from the excited quarks (U^+, U, D, D^-) of the quadruplet with $I_W = 3/2$.

One first thing to consider is that one of the two jets is from the heavy quark decay that makes it very energetic with a Jacobian peak in the transverse momentum spectrum near

$$p_T \approx (m_*/2)(1 - M_W^2/m_*^2) \qquad (18)$$

Using the p_T of the jets as a discriminant gives very good accuracy in identifying the jet coming from the decay of the heavy quark correctly, especially for high masses. Hence we identify the hardest jet (j1) in the event as the one from heavy quark decay.

We first define the transverse momentum of the highest p_T-jet as p_{Tj1}. The main kinematic feature of our signal process is the production of a very heavy excited quark U^+ with mass $m_* \approx \mathcal{O}$ (TeV). At very high masses it will then be a reasonable approximation to assume the exotic heavy particle to be produced nearly at rest. It will decay

in a pair of almost back to back high p_T jet and a high p_T W gauge boson. We expect both the p_{Tj1} and p_{TW} distributions to be peaked at $p_T \approx (m_*/2)(1 - M_W^2/m_*^2)$ and to be relatively similar in shape. These qualitative features are indeed confirmed by our numerical simulation of the signal distributions. Fig. 6 (bottom left and bottom right panels) show the p_{Tj1} and p_{TW} distributions for $m_* = 1000$ GeV which are clearly both peaked around $p_T \approx 400$ GeV in this case.

Fig. 6, Fig. 7, Fig. 8 and Fig. 9 show several normalized distributions with respect to both transverse momentum and angular variables. Fig 6 shows different transverse momentum distributions: the transverse momentum of the lepton $p_{T\ell}$, the second-leading $p_T(j2)$ and that of the leading p_{Tj1} are shown in Fig. 6(a,b,c) while the W gauge boson transverse p_T distribution is given in Fig. 6(d).

From the point of view of the transverse momentum distributions of the jets (leading and second-leading) in Fig. 6, signal and background are very well separated, for the given values of the parameters ($m_* = 1000$ GeV and $\Lambda = 10$ TeV). This suggests that a very efficient way we to reduce drastically the background while keeping most of the signal is a cut on the transverse momentum of the leading jet at ≈ 200 GeV and, possibly, a cut in the transverse momentum of the second-leading jet at ≈ 100 GeV.

From Fig. 7 we can see that both for the signal and the background a large fraction of the events have the two jets (or the lepton and the jets) with a large separation in the (η, ϕ) plane, $\Delta R = \sqrt{(\Delta\eta)^2 + (\Delta\phi)^2}$, ($\eta$ is the pseudorapidity and ϕ the azimuthal angle in the transverse plane). The corresponding ΔR distributions are peaked at $(\Delta R)_{\min} \approx 3$. Therefore, in the reconstruction process, the two jets can be easily separated as well as the lepton is cleary separated from the jets.
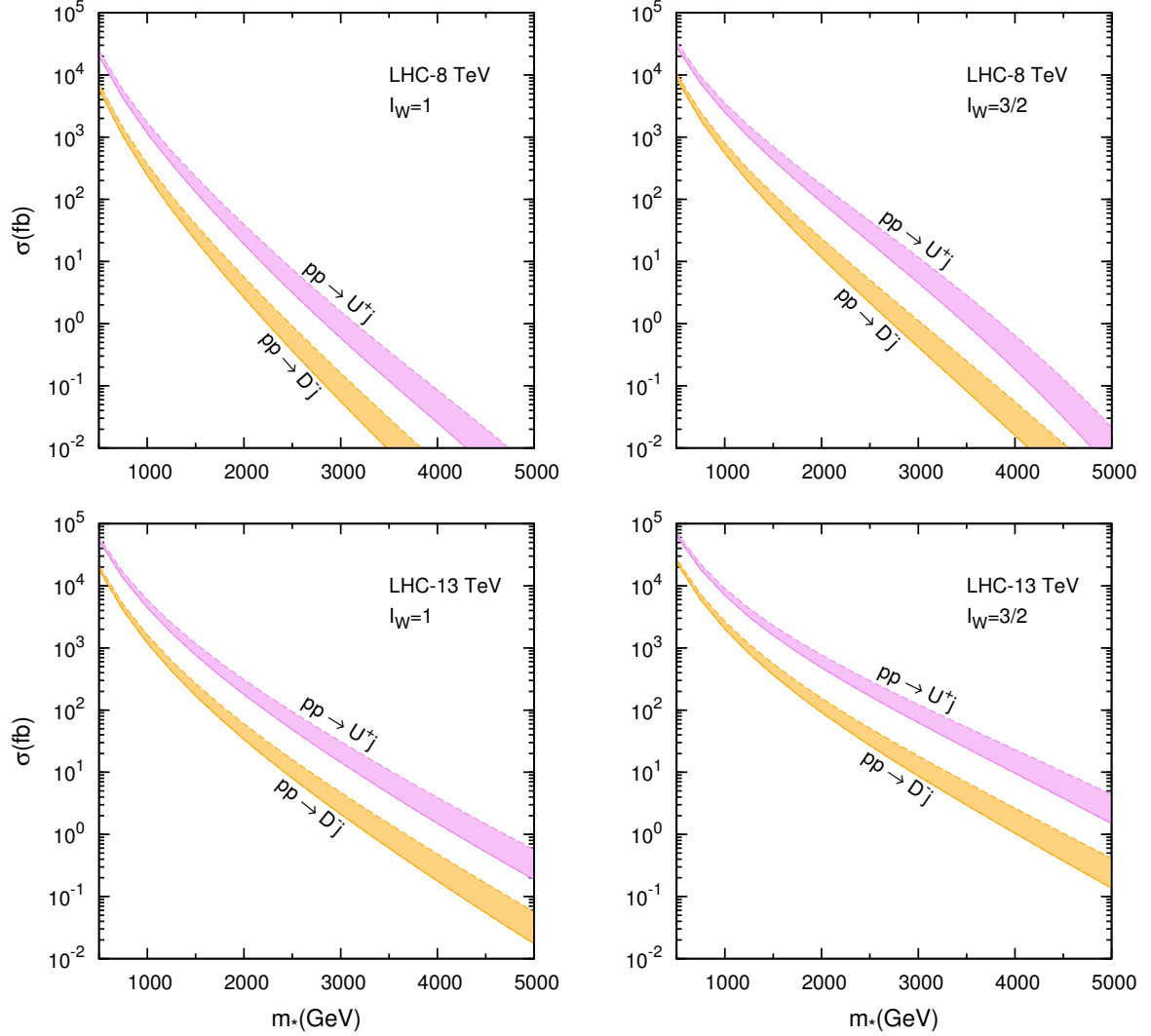
FIG. 5. (Color online) The total integrated cross-sections at the LHC energies of $\sqrt{s} = 8, 14$ TeV for the production of the exotic quarks U^+, of charge $Q = +(5/3)e$ and D^- of charge $Q = -(4/3)e$. We have used the NNPDF3.0 [58] parton distribution functions. The uncertainty bands (magenta and orange) correspond to running the factorization and renormalization scale from $\hat{\mathcal{Q}} = M_W$ (solid line) up to $\hat{\mathcal{Q}} = m_*$ (dashed line). All contributing sub-processes within the first two generations (18) have been summed up.

Differently than with the p_T distributions we can see from Fig. 8(a,b,c) that the pseudorapidity distributions of the leading jet in p_T, $\eta(j_1)$, and the second-leading jet in p_T, $\eta(j_2)$, and those of the lepton, $\eta(\ell)$, are quite similar for signal and background. The missing transverse energy distribution is shown Fig 8(d). Here signal and background are quite separated but we have checked that a cut on the missing transverse energy is less effective than one on the transverse momentum of the leading jet, $p_T(j_1)$.

Let us also comment on the fact that the $\ell \nu_\ell j j$ signature from a heavy composite quark state of charge $(+4/3)e$ has the potential to explain the excess observed in a search for 1st generation lepto-quarks (LQ) by the CMS collaboration [40] in the $e \not{p}_T j j$ invariant mass dis-

tribution in the interval $M_{ej} \approx 600$ GeV. Fig. 9 (a,b) shows, at the reconstructed level and for a particular point of the parameter space ($\Lambda = m_* = 1000$ GeV), that the $e j_1$ (electron and leading-jet) and $e j_2$ (electron and second-leading jet) invariant mass distribution can easily accomodate an excess in the interval where it has been claimed by the CMS collaboration. Our model would predict the same excess in the muon channel because the leptons arise from the decay of the W gauge boson. Some mechanism would have to be conceived in our model to suppress this excess in the muon channel. As already mentioned in the introduction we observe that this signature could also be affected by the production of an excited neutrino ($N = \nu^*$) in association with the corresponding lepton followed by the decay of the heavy
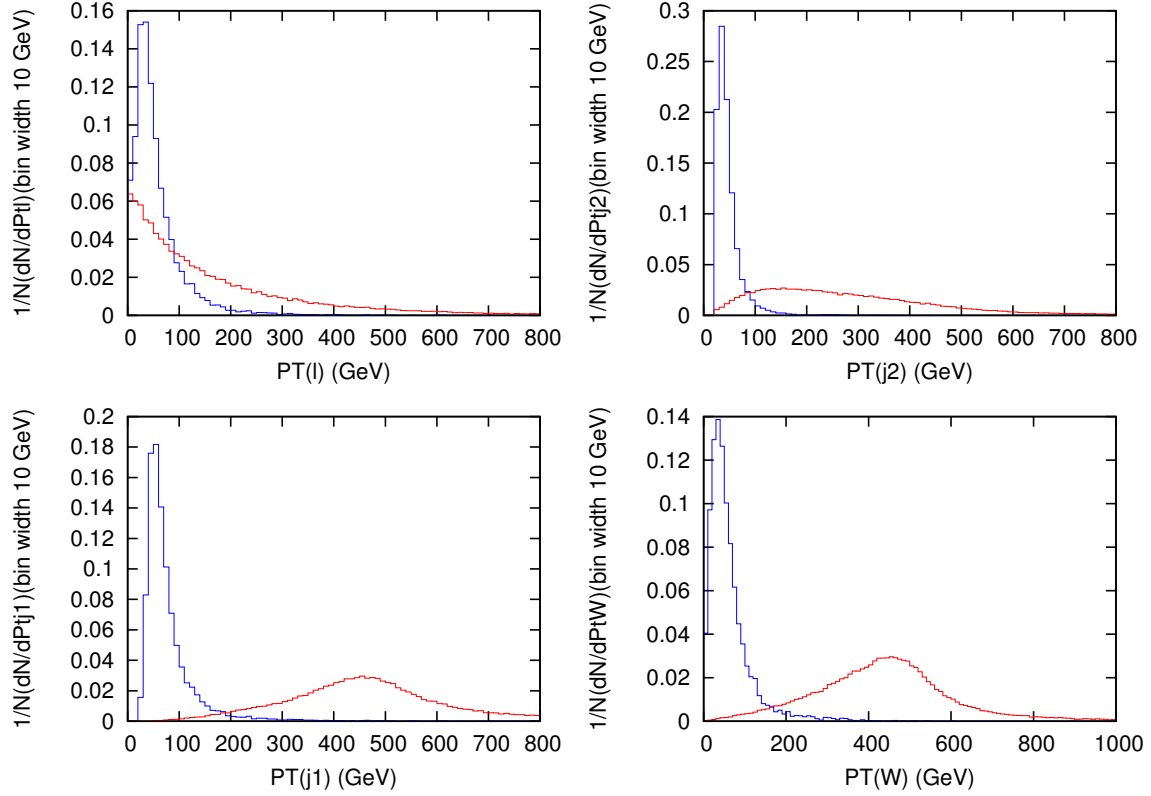
FIG. 6. (Color online) Transverse momentum distributions of the signal, light line (red), and of the SM background, dark line (blue): upper left panel, lepton distribution; upper right panel the second-leading jet distribution; lower left panel, leading jet and finally the W gauge boson transverse momentum distribution. These distributions clearly show that the most effective kinematic cut in order to optimize the statistical significance S is one on the p_T of the leading jet ($p_{Tj1} \approx O(200)$ GeV that will highly suppress the background while almost will not affect the signal. (d) Transverse p_T of the W gauge boson distribution of our signal $pp \to U^+ j \to W^+ j\, j$ superimposed with the standard model Wjj background.
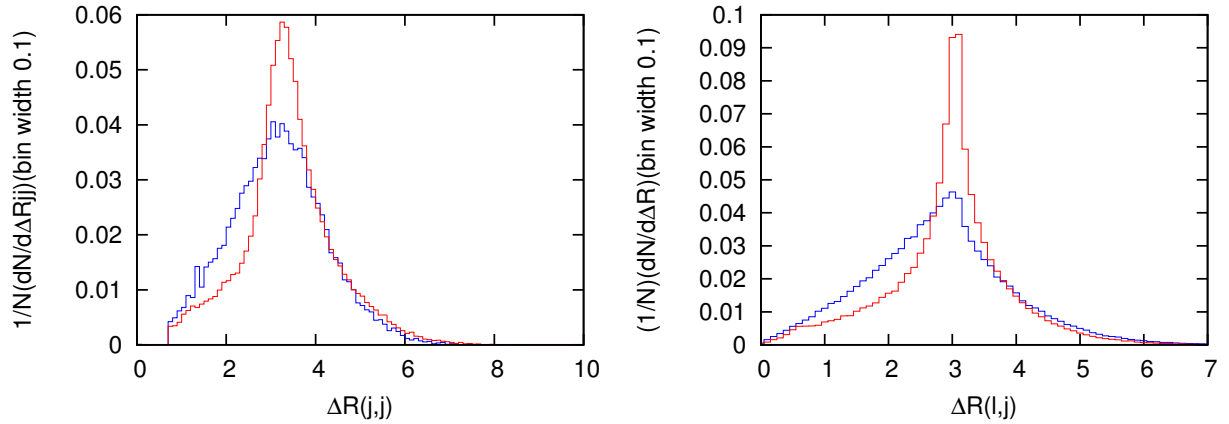

FIG. 7. (Color Online) Normalized ΔR distributions of signal, light line (red), and SM background, dark line (blue), clearly show that the two jets are well separated (plot on the left -ΔR_{jj}-) as well as the lepton and the jets (plot on the right -$\Delta R_{\ell j}$-).

neutrino to a lepton and a gauge boson decaying to two jets, thus obtaining $\ell \not{p}_T jj$. The differences in the electron and muon channels could then be ascribed to a mass hierarchy between the excited electron and muon heavy neutrinos.

We point out that within our final state signature ($\ell \nu_\ell jj$) it is always possible to define a *cluster* transverse mass variable (M_T) in terms of the reconstructed transverse momentum of the W gauge boson ($\boldsymbol{p}_{TW} = \boldsymbol{p}_{T\ell} + \boldsymbol{p}_{T\nu}$) and the transverse momentum of the leading
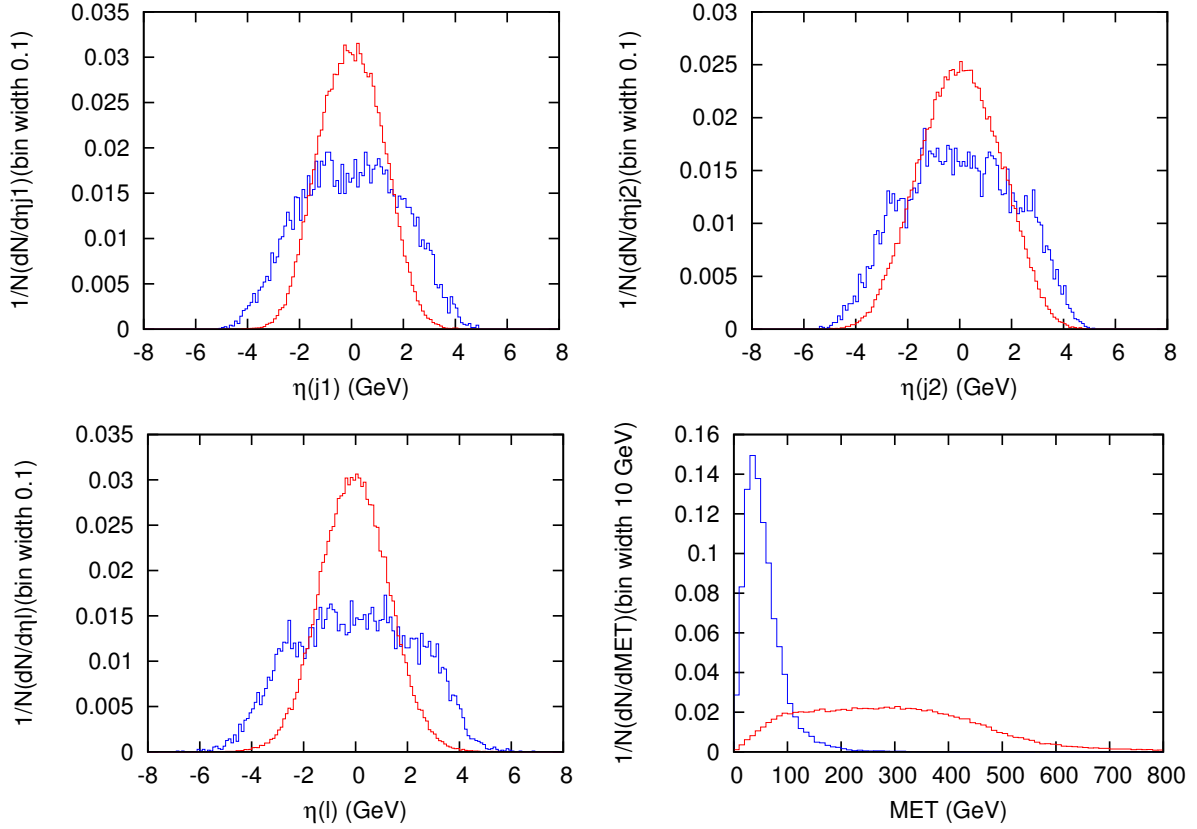
FIG. 8. (Color Online) Various (normalized) distributions of the signal $pp \to e\not{p}_T jj$, light line (red), in the case of an exotic quark state $U^+(5/3)$ mass $m_* = \Lambda = 1000$ GeV as well as of the SM background $pp \to Wjj \to \ell\not{p}_T jj$, dark line (blue), at $\sqrt{s} = 13$ TeV. We have used the NNPDF3.0 [58] parton distribution functions evaluated at the scale $\hat{Q} = m_*$. N.B. we have considered here all 14 subprocesses for a total of 29 Feynman diagrams within the first generation of quarks. In the top (left and right) panels and in the lower left panel we show respectively the pseudo-rapidity distributions of: (a) the highest p_T jet (j1); (b) the second-leading jet (j2); (c) the lepton. In the bottom right panel we show the missing transverse energy (MET) distribution.

jet (or highest p_T jet) p_{Tj_1}:

$$M_T^2 = \left(\sqrt{p_{TW}^2 + M_W^2} + p_{Tj1}\right)^2 - (\boldsymbol{p}_{TW} + \boldsymbol{p}_{Tj1})^2 \quad (19)$$

The transverse mass distribution is strongly correlated with the heavy exotic quark mass m_*. Relevant information about the mass of the heavy exotic quark U^+ can be obtained from the transverse mass distribution M_T. This is indeed the case as can be seen from Fig. 9(lower-left) where the transverse mass distribution obtained for the parameter value ($m_* = \Lambda = 1000$ GeV) shows a clear peak characterized by a relatively sharp end-point at $M_T \approx m_*$. This is expected since in the resonant production the heavy exotic quark, U^+ is decaying to $\ell\nu_\ell j$ and the jet from U^+ is expected to be the leading, while the second-leading jet is the one produced in association with U^+, in $pp \to U^+j$.

Finally we have also reconstructed the invariant mass distribution of the decay products of the heavy excited quark U^+: $\ell\nu_\ell j_1$. Indeed it is possible to reconstruct

the longitudinal neutrino momentum $p_z(\nu)$ up to a two-fold ambiguity [59]. The resulting reconstructed invariant mass $M_{\ell\nu j_1}$ is shown in Fig. 9(lower-right).

In order to still reconstruct the invariant mass of the exotic quark to some degree of accuracy, we can follow the method described in [59] modified to adatpt it to our case. We use the conservation of four-momentum to solve for the longitudinal momentum of the neutrino (p_L^ν). Conservation of four-momentum, $p_W = p_\ell + p_\nu$, gives the following equation:

$$M_W^2 = (p_\ell + p_\nu)^2. \quad (20)$$

The only unknown quantity in Eq. 20 is the longitudinal momentum of the neutrino. Expanding the right-hand side of Eq. 20 we obtain a second-order equation for p_L^ν:

$$(1 - B^2)(p_L^\nu)^2 - 2A\,B\,p_T^\nu p_L^\nu + (p_T^\nu)^2(1 - A^2) = 0 \quad (21)$$

where $p_T^\nu = |\boldsymbol{p}_T^\nu|$ while p_L^ν and p_L^ℓ are the true components (with sign) of the neutrino and lepton momentum along
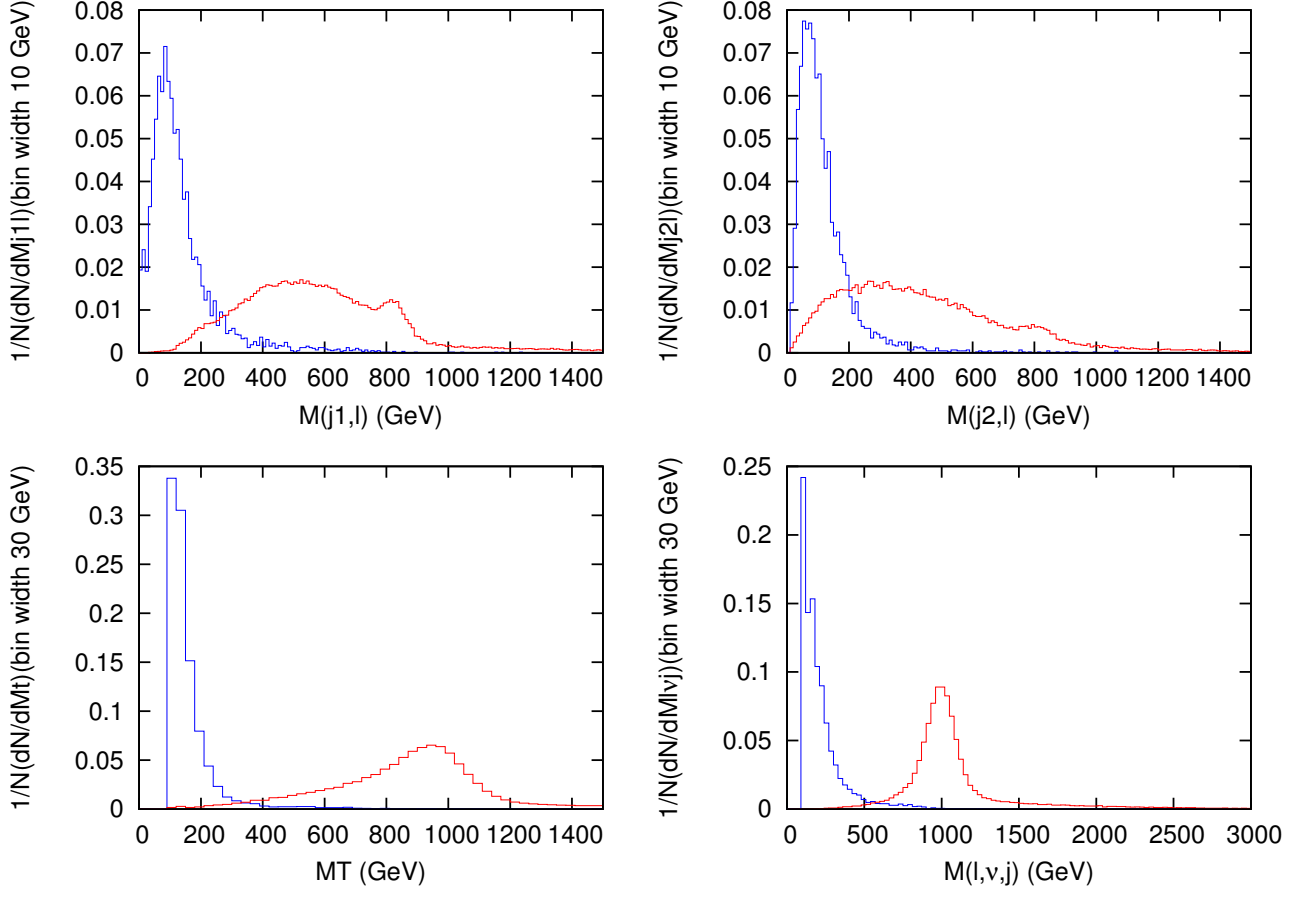
FIG. 9.   (Color online) Various invariant and transverse mass distributions for a choice of $m_* = \Lambda = 1000$ GeV at $\sqrt{s} = 13$ TeV for the signal, light line (red), and the SM background, dark line (blue). In the top left and top right panels we show the invariant mass distribution of the lepton with j_1 the highest p_T jet (leading) and with j_2 the second leading jet. In the bottom panels we show the transverse mass M_T distribution (left) and the reconstructed invariant mass, $M(\ell\nu_\ell j_1)$, of the decay products of the exotic quark U^+ (right).

the (longitudinal) z-axis and:

$$A = \frac{M_W^2 + 2\, \boldsymbol{p}_T^\ell \cdot \boldsymbol{p}_T^\nu}{2E_\ell p_T^\nu}, \qquad B = \frac{p_L^\ell}{E_\ell}. \qquad (22)$$

It has the solutions:

$$p_L^\nu = \frac{1}{1 - B^2} \left[AB \pm \sqrt{A^2 + B^2 - 1} \right] p_\nu^T \qquad (23)$$

Note that the discriminant (D) of the second order equation is the quantity in the square root, $D = A^2 + B^2 - 1$. We have three distinct possibilities: (i) $D > 0$, two real solutions; (ii) $D = 0$, one real solution; (iii) $D < 0$, two complex solutions.

If the discriminant is zero there is only one solution for p_L^ν which can be used to fully reconstruct the neutrino. If the discriminant is negative, the event is rejected. If the discriminant is positive, there are two possible p_L^ν solutions. Using both of them, the two possible neutrino momentum vectors are constructed and, combining them with the lepton momentum, the two W candidate are re-constructed. We select the p_L^ν solution that

gives the more central W, i.e. with the smaller pseudo-rapidity. Then we can reconstruct the corresponding invariant mass $M_{\ell\nu_\ell j1}$. Fig. 9 shows the distribution in the invariant mass of the lepton, jet and neutrino. There is a clear peak in correspondence of the exotic quark mass.

V.   FAST DETECTOR SIMULATION AND RECONSTRUCTED OBJECTS

In order to take into account the detector effects, such as efficiency and resolution in reconstructing kinematic variables, we interface the LHE output of CalcHEP with the software DELPHES that simulates the response of a generic detector according to predefined configurations. We use a CMS-like parametrization. For the signal we consider a scan of the parameter space $(\Lambda = m_*)$ within the range $m_* \in [500, 5000]$ GeV with step of 500 GeV. We have studied four different choices of kinematical cuts $t_1 \ldots t_4$ as described in Table III. Although the various choices perform quite similarly, it turns out that the most

cut	$p_T(j1)$	$p_T(j2)$	M_T
t_1	$> 180\,\mathrm{GeV}$	$-$	$-$
t_2	$> 200\,\mathrm{GeV}$	$-$	$-$
t_3	$> 180\,\mathrm{GeV}$	$> 100\,\mathrm{GeV}$	$-$
t_4	$> 180\,\mathrm{GeV}$	$-$	$> 400\,\mathrm{GeV}$

TABLE III. Various cuts which have been studied in order to maximise the statistical significance. It turns out that cut t_3 is the most efficient cut.

efficient choice is found to be cut t_3:

$$p_T(j_{\text{leading}}) \geq 180\,\text{GeV}, \tag{24a}$$
$$p_T(j_{\text{second-leading}}) \geq 100\,\text{GeV}. \tag{24b}$$

For each signal point and for the standard model background we generate 10^5 events in order to have enough statistics to evaluate the reconstruction efficiencies (ϵ_s, ϵ_b) of the detector and of the cuts previously fixed (see Eq. 24a, 24b). We select the events with two jets, one lepton and $\not{p}_T$ in the final state. This is justified because the two jets are well separated, as opposed for instance to what happens the signal $pp \to \ell\ell jj$ studied in ref. [37], due to a heavy composite Majorana neutrino, where it was found that depending on the heavy neutrino mass (m_*) it is possible to have merging of the two jets in a sizeable fraction of the events. Once we have the number of the selected events we evaluate the reconstruction efficiencies. The efficiencies are shown for the choice of cuts t_3 (see Table III) in Table IV. Then for a given luminosity L it is possible to estimate the expected number of events for the signal (N_s) and for the background (N_b):

$$N_s = L\sigma_s\epsilon_s, \qquad N_b = L\sigma_b\epsilon_b, \tag{25}$$

and finally the statistical significance (S) is evaluated as:

$$S = \frac{N_s}{\sqrt{N_s + N_b}}. \tag{26}$$

It is then possible to obtain the luminosities needed to obtain an effect of a given statistical significance as :

$$L = \frac{S^2}{\sigma_s\epsilon_s}\left[1 + \frac{\sigma_b\epsilon_b}{\sigma_s\epsilon_s}\right] \tag{27}$$

Therefore luminosity curves at 5- and 3-σ level (i.e. fixing $S = 3$ or $S = 5$) can be straightforwardly given as a function of the mass m_* of the exotic quark. Fig. 10 shows such 3- and 5 sigma luminosity curves which can also be used to get indications on the potential for discovery (or exclusion) at a given luminosity reached by the experiments at Run II of the LHC.

We conclude this section by providing a discussion of the bounds on the excited quarks of extended weak isospin multiplets $I_W = 1, 3/2$ by recasting preliminary results on a search for exotic light flavour quark partners in pp collisions at $\sqrt{s} = 8$ TeV, [60] with a data sample of

Background		
σ_b before cut (fb)	σ_b after cut (fb)	(ϵ_b)
8200000	14678	0.00179
Signal ($I_W = 1$)		
m_* (GeV) $\mid$ σ_s before cut (fb)	σ_s after cut (fb)	(ϵ_s)
500 $\mid$ 19358	12213.1	0.630906
1000 $\mid$ 2941.7	2367.87	0.804931
1500 $\mid$ 758.69	643.786	0.848549
2000 $\mid$ 233.98	203.191	0.868412
2500 $\mid$ 81.653	71.5896	0.876754
3000 $\mid$ 29.579	26.1131	0.882824
3500 $\mid$ 9.7124	8.6383	0.88941
4000 $\mid$ 3.2272	2.87522	0.890934
4500 $\mid$ 1.11613	0.994357	0.890897
5000 $\mid$ 0.4045	0.362569	0.896339
Signal ($I_W = 3/2$)		
m_* (GeV) $\mid$ σ_s before cut (fb)	σ_s after cut (fb)	(ϵ_s)
500 $\mid$ 16509.6	8888.19	0.538365
1000 $\mid$ 3062.46	2257.67	0.737208
1500 $\mid$ 1047.05	841.233	0.803432
2000 $\mid$ 434.357	358.925	0.826336
2500 $\mid$ 202.911	169.963	0.837622
3000 $\mid$ 84.9877	73.1053	0.860187
3500 $\mid$ 32.2702	27.4566	0.850835
4000 $\mid$ 11.4527	9.31689	0.813507
4500 $\mid$ 3.84621	3.13297	0.814562
5000 $\mid$ 1.2537	1.01801	0.812003

TABLE IV. Efficiencies of the standard model Wjj background and of our signature for the $I_W = 3/2$ and $I_W = 1$ cases. The estimated efficiencies refer to the choice of kinematic cut t_3 described in Tab. III or Eqs. 24a, 24b.

19.6 fb^{-1}. By comparing the 95% confidence level (C.L.) observed limit on $\sigma(pp \to Dq) \times \mathcal{B}(D \to Zq)$ with the prediction of our composite scenario with a triplet ($I_W = 1$) or a quadruplet ($I_W = 3/2$) we can estimate the bound on our model parameter $m_* = \Lambda$. It turns out that for $I_W = 1$ $m_* > 1550$ GeV while for $I_W = 3/2$, $m_* > 1710$ GeV. See Fig. 11 for details. This is, to the best of our knowledge, the first estimate of a bound on the mass of the excited quarks belonging to extended weak iso-spin multiplets discussed originally in [12] from existing data. We note that in ref. [60] 95% C. L. limits are also provided for the charged channel (Wqq) in the same mass window as in Fig. 11. However the theoretical prediction of our model would cross the 95% C. L. observed limit on $\sigma(pp \to Dq) \times \mathcal{B}(D \to Wq)$ outside of the mass window of the data. We have therefore decided to drop this channel.

VI. CONCLUSIONS

We have presented the first study of the production at the CERN LHC of new exotic quark states of charge $Q = +(5/3)e$ and $Q = -(4/3)e$ which appear in composite models of quarks and leptons when considering higher isospin multiplets $I_W = 1$ and $I_W = 3/2$. Such states have been discussed quite sometime back [12] but their
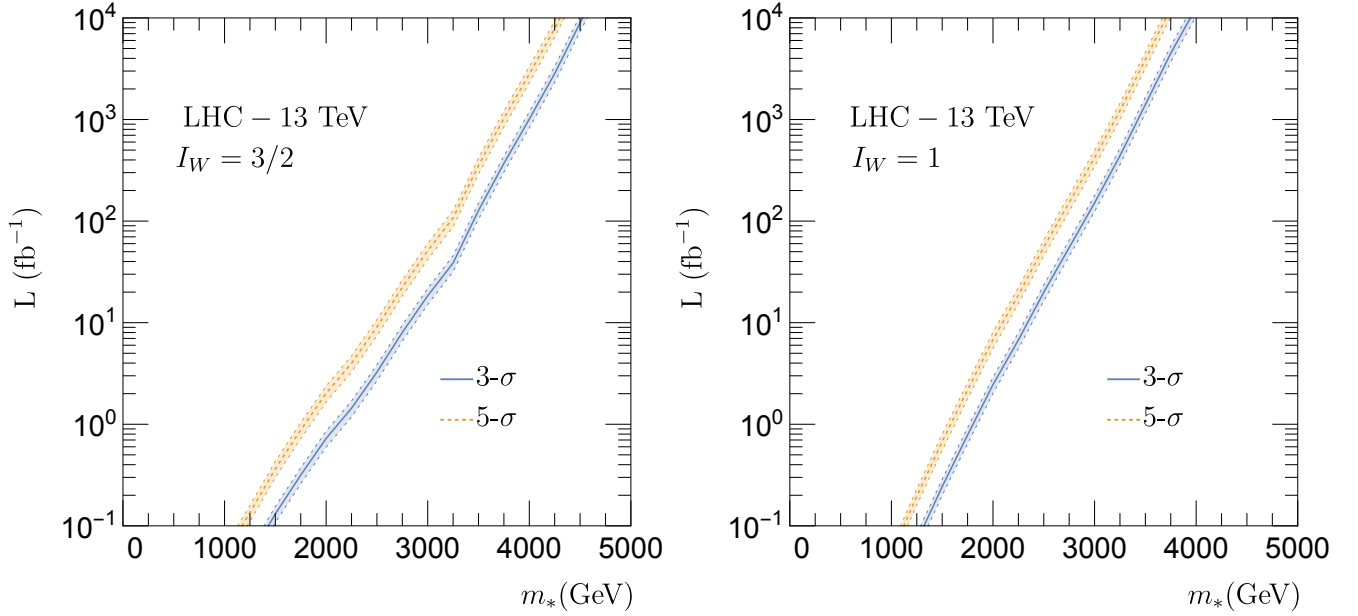
FIG. 10. (Color online) Luminosity curves at 3-σ (solid) and 5-σ (dashed) level for $\sqrt{s} = 13$ TeV as a function of the excited quark mass m_* after including the fast simulation efficiencies of the detector reconstruction. For $I_W = 1$, and for values of the integrated luminosity equal to $L = (30, 300, 3000)$ fb^{-1} we find a 3-sigma level mass reach respectively up to $m_* \approx (2570, 3130, 3630)$ GeV. For the same values of the integrated luminosity in the $I_W = 3/2$ case we find a 3-sigma level mass reach respectively up to $m_* \approx (3140, 3730, 4260)$ GeV. The shaded bands around the solid (3-σ) and dashed (5-σ) lines define the luminosity curves within the statistical error.

phenomenology has been, somewhat surprisingly, not addressed in detail. Only very recently [34–36] some attention has been devoted to the phenomenology of exotic doubly charged states appearing in the lepton sector of the extended weak isospin model of ref. [12]. Here we explore, to the best of our knowledge for the first time, the phenomenology of the hadron sector of the same model with respect to the CERN LHC experiments, with a focus on the Run II at a center of mass energy of $\sqrt{s} = 13$ TeV. This is one of the motivations which started the present work. Although the excited quark model alone cannot provide a (qualitative) explanation for an excess in the $e \not{p}_T j j$ channel with no excess in the $\mu \not{p}_T j j$ channel [41, 42], a composite model with excited leptons, with non-flavor universal masses and/or non-flavor-universal couplings to the SM leptons might explain this combination of signals, as some of the authors suggested previously [37].

This is particularly interesting in view of the fact that the recent studies [37] of the lepton sector of extended weak-isospin composite multiplets suggest a possible explanation of the concomitant CMS excess observed in the $eejj$ channel [40] in terms of an hypothetical composite Majorana neutrino. In [37] it has been also suggested that the composite scenario could also be connected to the recent anomaly reported by the ATLAS collaboration in a search of resonances in the di-boson channel [61].

In our study of the Wqq final state (actually $\ell \not{p}_T j j$) we have included the dominant contribution from the quark partners of charge 5/3 and 4/3 $U^+, \bar{D}^-$, as well as the contributions from the states of ordinary charge +2/3 and -1/3, the quarks U, D. See Tables I&II. We typically find that the U, D contributions account for a fraction of the total yield that depends oon the mass m_* and ranges from 30-40% at low masses and goes down to about 20% at large masses.

We have implemented the magnetic type Gauge interactions in the CalcHEP generator and performed a fast simulation of the detector reconstruction of both signal and relevant SM background (Wjj) based on the DELPHES software [43].

We compute the luminosity curves as functions of m_* for 3- and 5-σ level statistical significance including the statistical error. For different values of the integrated luminosity $L = (30, 300, 3000)$ fb^{-1} we find for instance that, for $I_W = 3/2$ we can either observe or exclude (at a 3-σ level) respectively masses up to

L (fb^{-1})	3-σ m_* (GeV)	5-σ m_* (GeV)
30	$3140 + 70 - 50$	$2820 + 50 - 40$
300	$3730 + 40 - 50$	$3450 + 50 - 50$
3000	$4260 + 30 - 50$	$4035 + 30 - 30$

TABLE V. Discovery reach, in the case $I_W = 3/2$, for m_* at 3- and 5-σ level within the statistical error at different values of the integrated luminosity $L = (30, 300, 3000)$ fb^{-1}.
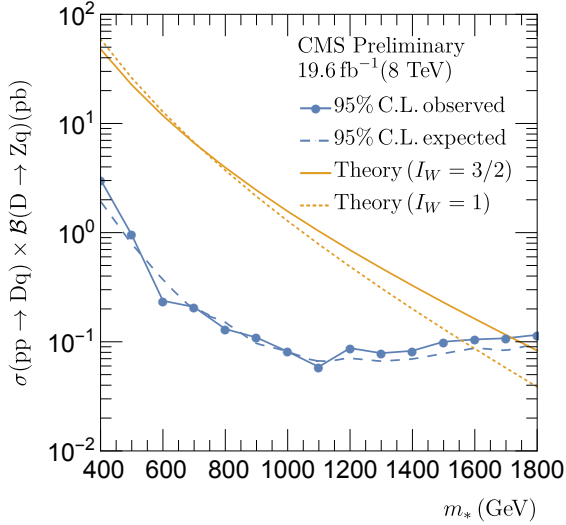
FIG. 11. (Color online) 95% Confidence Level limits observed (solid line with disk markers) and expected (dashed line) as reported by a CMS search [60] for light flavour quark partners in the Zqq channel with the prediction of our model are compared with predictions from our theoretical model. For $I_W = 3/2$, solid line (orange) masses lower than $m_* \approx 1710$ GeV are excluded at 95% C.L. while for $I_W = 1$, dotted line (orange), the lower bound is $m_* \approx 1550$ GeV.

L (fb^{-1})	3-σ m_* (GeV)	5-σ m_* (GeV)
30	$2570 + 50 - 30$	$2330 + 40 - 30$
300	$3130 + 50 - 40$	$2890 + 60 - 40$
3000	$3630 + 50 - 40$	$3420 + 60 - 50$

TABLE VI. Discovery reach, in the case $I_W = 1$, for m_* at 3- and 5-σ level within the statistical error at different values of the integrated luminosity $L = (30, 300, 3000)$ fb^{-1}.

Finally we have also estimated a bound on the mass of the excited quarks of our composite scenario with extended weak iso-spin multiplets comparing predictions of our models ($I_W = 1$, and $I_W = 3/2$) against published data from a CMS search [60] of exotic light flavour quark partners in pp collisions at $\sqrt{s} = 8$ TeV at LHC. Our analysis shows that typical lower bounds on the mass of excited quarks from extended weak iso-spin models would be around $m_* \approx 1710$ GeV for $I_W = 3/2$ and $m_* \approx 1550$ GeV for $I_W = 1$ based on the 95 confidence level observed limits in the Zqq channel.

The above are quite interesting results which in our opinion warrant more detailed studies. For instance the two dimensional parameter space (Λ, m_*) could be fully explored. Also the effect of expected contact interactions should be taken into account. This could improve the sensitivity of the signature to larger portions of the parameter space.

ACKNOWLEDGMENTS

$m_* \approx (3140, 3730, 4260)$ GeV. See table V & VI for details.

[1] P. A. M. Dirac, Scientific American **208**, 45 (1963).
[2] H. Terazawa, K. Akama, and Y. Chikashige, Phys.Rev. **D15**, 480 (1977).
[3] H. Terazawa, Phys.Rev. **D22**, 184 (1980).
[4] E. Eichten and K. Lane, Physics Letters B **90**, 125 (1980).
[5] E. Eichten, K. D. Lane, and M. E. Peskin, Phys. Rev. Lett. **50**, 811 (1983).
[6] H. Terazawa, in *Europhysics Topical Conference: Flavor Mixing in Weak Interactions Erice, Italy, March 4-12, 1984* (1984).
[7] N. Cabibbo, L. Maiani, and Y. Srivastava, Phys. Lett. **B139**, 459 (1984).
[8] U. Baur, M. Spira, and P. M. Zerwas, Phys. Rev. D **42**, 815 (1990).
[9] U. Baur, I. Hinchliffe, and D. Zeppenfeld, Int. J. Mod. Phys. **A2**, 1285 (1987).
[10] G. Aad *et al.* (ATLAS Collaboration), Phys. Rev. Lett. **105**, 161801 (2010).
[11] G. Aad *et al.* (ATLAS), JHEP **02**, 110 (2016), arXiv:1510.02664 [hep-ex].
[12] G. Pancheri and Y. N. Srivastava, Phys. Lett. **B146**, 87 (1984).
[13] O. Matsedonskyi, G. Panico, and A. Wulzer, JHEP **04**, 003 (2016), arXiv:1512.04356 [hep-ph].
[14] F. D. Aguila and M. Bowick, Nuclear Physics B **224**, 107 (1983).
[15] J. A. Aguilar-Saavedra, Journal of High Energy Physics **2009**, 030 (2009).
[16] J. A. Aguilar-Saavedra, EPJ Web of Conferences **60**, 16012 (2013).
[17] J. A. Aguilar-Saavedra, R. Benbrik, S. Heinemeyer, and M. Pérez-Victoria, Phys. Rev. D **88**, 094010 (2013).
[18] D. Barducci, A. Belyaev, M. Buchkremer, J. Marrouche, S. Moretti, and L. Panizzi, Computer Physics Communications **197**, 263 (2015).
[19] D. Barducci, A. Belyaev, M. Buchkremer, G. Cacciapaglia, A. Deandrea, S. De Curtis, J. Marrouche,

S. Moretti, and L. Panizzi, JHEP **12**, 080 (2014), arXiv:1405.0737 [hep-ph].

[20] G. Cacciapaglia, A. Deandrea, N. Gaur, D. Harada, Y. Okada, and L. Panizzi, JHEP **09**, 012 (2015), arXiv:1502.00370 [hep-ph].

[21] R. Contino and G. Servant, JHEP **06**, 026 (2008), arXiv:0801.1679 [hep-ph].

[22] A. Atre, G. Azuelos, M. Carena, T. Han, E. Ozcan, J. Santiago, and G. Unel, JHEP **08**, 080 (2011), arXiv:1102.1987 [hep-ph].

[23] S. Chatrchyan *et al.* (CMS Collaboration), Phys. Rev. Lett. **112**, 171801 (2014).

[24] *Search for top quark partners with charge 5/3 at $\sqrt{s} = 13$ TeV*, Tech. Rep. CMS-PAS-B2G-15-006 (CERN, Geneva, 2015).

[25] A. M. Sirunyan *et al.* (CMS Collaboration), (2017), arXiv:1705.10967 [hep-ex].

[26] V. Khachatryan, A. M. Sirunyan, A. Tumasyan, *et al.* (CMS Collaboration), Phys. Rev. Lett. **105**, 211801 (2010).

[27] *Search for narrow resonances decaying to dijets in pp collisions at $\sqrt{s} = 13$ TeV using 12.9 fb^{-1}*, Tech. Rep. CMS-PAS-EXO-16-032 (CERN, Geneva, 2016).

[28] A. M. Sirunyan *et al.* (CMS Collaboration), Physics Letters B **769**, 520 (2017).

[29] V. Khachatryan *et al.* (CMS Collaboration), Phys. Rev. Lett. **116**, 071801 (2016).

[30] G. Aad *et al.*, Physics Letters B **754**, 302 (2016).

[31] S. Bhattacharya, S. S. Chauhan, B. C. Choudhary, and D. Choudhury, Phys. Rev. D **76**, 115017 (2007).

[32] S. Bhattacharya, S. S. Chauhan, B. C. Choudhary, and D. Choudhury, Phys. Rev. D **80**, 015014 (2009).

[33] T. Golling, Progress in Particle and Nuclear Physics **90**, 156 (2016).

[34] S. Biondini, O. Panella, G. Pancheri, Y. Srivastava, and L. Fanò, Phys. Rev. D **85**, 095018 (2012), arXiv:1201.3764 [hep-ph].

[35] R. Leonardi, O. Panella, and L. Fanò, Phys. Rev. D **90**, 035001 (2014).

[36] S. Biondini and O. Panella, Phys. Rev. D **92**, 015023 (2015).

[37] R. Leonardi, L. Alunni, F. Romeo, L. Fanò, and O. Panella, The European Physical Journal C **76**, 593 (2016).

[38] *Search for heavy composite Majorana neutrinos produced in association with a lepton and decaying into a same-flavour lepton plus two quarks at $\sqrt{s} = 13$ TeV with the CMS detector*, Tech. Rep. CMS-PAS-EXO-16-026 (CERN, Geneva, 2016).

[39] A. M. Sirunyan *et al.* (CMS Collaboration), (2017), arXiv:1706.08578 [hep-ex].

[40] V. Khachatryan *et al.* (CMS Collaboration), Eur.Phys.J. **C74**, 3149 (2014), arXiv:1407.3683 [hep-ex].

[41] *Search for Pair-production of First Generation Scalar Leptoquarks in pp Collisions at sqrt s = 8 TeV*, Tech. Rep. CMS-PAS-EXO-12-041 (CERN, Geneva, 2014).

[42] V. Khachatryan *et al.* (CMS Collaboration), Phys. Rev. D **93**, 032004 (2016).

[43] J. de Favereau *et al.* (DELPHES 3), JHEP **1402**, 057 (2014), arXiv:1307.6346 [hep-ex].

[44] G. Aad and L. Zwalinski, New Journal of Physics **15**, 093011 (2013).

[45] *Search for excited leptons in proton proton collisions at $\sqrt{s} = 8$ TeV*, Tech. Rep. CMS-PAS-EXO-14-015 (CERN, Geneva, 2015).

[46] V. Khachatryan *et al.* (CMS Collaboration), Journal of High Energy Physics **2016**, 125 (2016).

[47] M. Buchkremer, G. Cacciapaglia, A. Deandrea, and L. Panizzi, Nucl. Phys. **B876**, 376 (2013), arXiv:1305.4172 [hep-ph].

[48] A. De Simone, O. Matsedonskyi, R. Rattazzi, and A. Wulzer, JHEP **04**, 004 (2013), arXiv:1211.5663 [hep-ph].

[49] A. Pukhov, (2004), arXiv:hep-ph/0412191.

[50] N. D. Christensen and C. Duhr, Comput. Phys. Commun. **180**, 1614 (2009), arXiv:0806.4194 [hep-ph].

[51] A. S. Belyaev, E. E. Boos, and L. V. Dudko, Phys. Rev. **D59**, 075001 (1999), arXiv:hep-ph/9806332.

[52] A. Belyaev, E. Boos, L. Dudko, and A. Pukhov, (1995), arXiv:hep-ph/9511306.

[53] D. Eriksson, S. Hesselbach, and J. Rathsman, Eur. Phys. J. **C53**, 267 (2008), arXiv:hep-ph/0612198.

[54] D. Eriksson, S. Hesselbach, and J. Rathsman, (2007), arXiv:0710.3346 [hep-ph].

[55] F. Renard, Physics Letters B **116**, 264 (1982).

[56] M. Gonzalez-Garcia and S. Novaes, Physics Letters B **389**, 707 (1996).

[57] M. Gonzalez-Garcia and S. Novaes, Nuclear Physics B **486**, 3 (1997).

[58] R. D. Ball, V. Bertone, S. Carrazza, C. S. Deans, L. Del Debbio, S. Forte, A. Guffanti, N. P. Hartland, J. I. Latorre, J. Rojo, and M. Ubiali, Journal of High Energy Physics **04**, 040 (2015).

[59] S. Richter, *Invariant mass reconstruction in a search for light charged Higgs bosons in pp collisions at $\sqrt{s} = 7$ TeV*, Master's thesis, Helsinki U. (2013).

[60] *Search for exotic light-flavor quark partners in pp collisions at $\sqrt{s} = 8$ TeV*, Tech. Rep. CMS-PAS-B2G-12-016 (CERN, Geneva, 2016).

[61] G. Aad *et al.* (ATLAS), JHEP **12**, 055 (2015), arXiv:1506.00962 [hep-ex].